Article

Cell

Causal Influence of Visual Cues on Hippocampal Directional Selectivity

Graphical Abstract

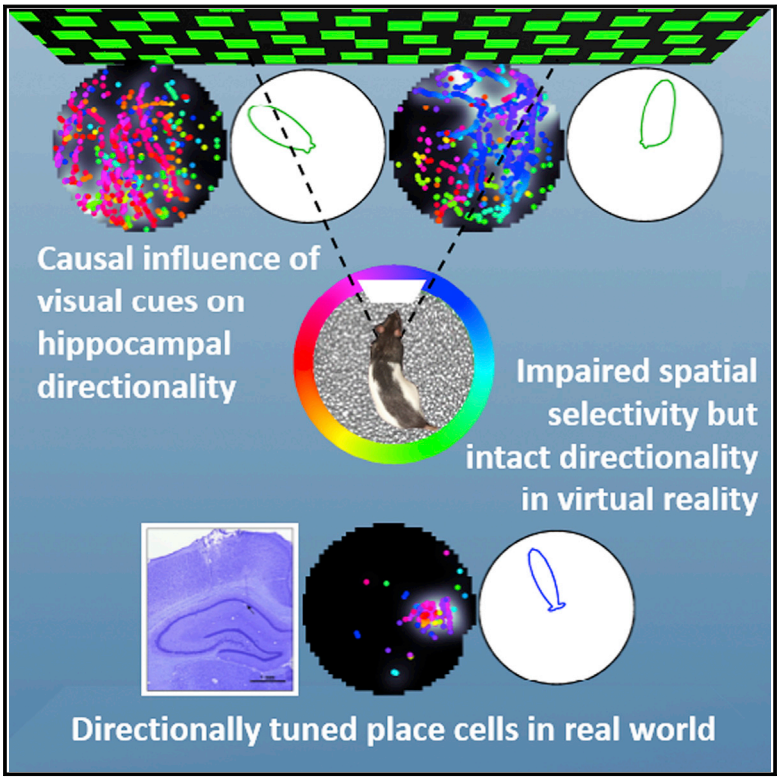

Highlights

- Hippocampal neurons exhibit head-directional modulation in 2D real-world arenas
- Significant head-directional modulation is also present in virtual reality
- Visual cues exert a causal influence on hippocampal neuronal and ensemble activity
- Vestibular cues are not required for the generation of hippocampal directionality

Authors

Lavanya Acharya, Zahra M. Aghajan, Cliff Vuong, Jason J. Moore, Mayank R. Mehta

Correspondence

mayankmehta@ucla.edu

In Brief

Virtual reality and real-world electrophysiology measurements demonstrate that more than a quarter of rodent hippocampal neurons are modulated in a causal and predictable manner by the animal's head direction with respect to visual cues, thus challenging long-held beliefs on directionality.

Acharya et al., 2016, Cell *164*, 197–207
January 14, 2016
http://dx.doi.org/10.1016/j.cell.2015.12.015

CellPress

Article

Cell

Causal Influence of Visual Cues on Hippocampal Directional Selectivity

Lavanya Acharya,[1,2,6] Zahra M. Aghajan,[1,3,6] Cliff Vuong,[1,3] Jason J. Moore,[1,4] and Mayank R. Mehta[1,3,4,5,*]

[1]W.M. Keck Center for Neurophysics, Integrative Center for Learning and Memory, and Brain Research Institute, University of California at Los Angeles, Los Angeles, CA 90095, USA

[2]Biomedical Engineering Interdepartmental Program, University of California at Los Angeles, Los Angeles, CA 90095, USA

[3]Department of Physics and Astronomy, University of California at Los Angeles, Los Angeles, CA 90095, USA

[4]Neuroscience Interdepartmental Program, University of California at Los Angeles, Los Angeles, CA 90095, USA

[5]Departments of Neurology and Neurobiology, University of California at Los Angeles, Los Angeles, CA 90095, USA

[6]Co-first author

*Correspondence: mayankmehta@ucla.edu

http://dx.doi.org/10.1016/j.cell.2015.12.015

SUMMARY

Hippocampal neurons show selectivity with respect to visual cues in primates, including humans, but this has never been found in rodents. To address this long-standing discrepancy, we measured hippocampal activity from rodents during real-world random foraging. Surprisingly, ~25% of neurons exhibited significant directional modulation with respect to visual cues. To dissociate the contributions of visual and vestibular cues, we made similar measurements in virtual reality, in which only visual cues were informative. Here, we found significant directional modulation despite the severe loss of vestibular information, challenging prevailing theories of directionality. Changes in the amount of angular information in visual cues induced corresponding changes in head-directional modulation at the neuronal and population levels. Thus, visual cues are sufficient for—and play a predictable, causal role in—generating directionally selective hippocampal responses. These results dissociate hippocampal directional and spatial selectivity and bridge the gap between primate and rodent studies.

INTRODUCTION

The hippocampus has been implicated in navigation, for which both spatial and directional information are necessary. Hippocampal spatial selectivity has been well established, and the underlying mechanisms have been extensively studied (Andersen et al., 2006; O'Keefe and Dostrovsky, 1971; O'Keefe and Nadel, 1978). However, rodent hippocampal neurons are commonly believed to have no directional selectivity in two-dimensional mazes (Andersen et al., 2006; Muller et al., 1994). This has led to a hypothesis that the directional information is not available in the hippocampus but is instead provided by other parts of the brain, such as the head-direction nuclei. Further, the sensory mechanisms underlying directionality are debated, though vestibular and visual cues are thought to be crucial (Knierim et al., 1995; Markus et al., 1995; Ravassard et al., 2013). In addition, internal mechanisms also contribute to hippocampal activity (Aghajan et al., 2015; MacDonald et al., 2011; Pastalkova et al., 2008; Peyrache et al., 2015).

Visual cues strongly influence the spatial firing properties of hippocampal neurons (Muller and Kubie, 1987; Shapiro et al., 1997). For example, changes (Shapiro et al., 1997) and rotations (Muller and Kubie, 1987) of visual cues cause remapping or rotation, respectively, of some place fields. Further, unlike two-dimensional mazes, on one-dimensional mazes hippocampal neurons exhibit strong directional selectivity (Battaglia et al., 2004; Markus et al., 1995; McNaughton et al., 1983; Ravassard et al., 2013). The reasons for this disparity are unknown. Comparable levels of directionality exist on linear tracks in real world (RW) and in virtual reality (VR) (Ravassard et al., 2013)—where the range of rotational vestibular inputs is minimal and visual cues are the only directionally informative cues—suggesting that visual cues also support directionality in one dimension. In addition, selectivity to the visual cue toward which the animal's head is facing, referred to as spatial view, has been reported in humans (Ekstrom et al., 2003), primates (Rolls and O'Mara, 1995; Rolls, 1999), and bats (Ulanovsky and Moss, 2011). However, response to specific features of visual cues has not been observed in rodents, and spatial selectivity persists in darkness, leading to the notion that, in these animals, visual cues merely provide a context for hippocampal activity.

In parallel, vestibular inputs are crucial to the head-direction system, which is thought to provide directional information to the hippocampus. Consistently, vestibular lesions disrupt hippocampal spatial selectivity (Stackman et al., 2002), although lesions in the head-direction system do not (Calton et al., 2003). Some studies have attributed directionality in two dimensions to vestibular-derived self-motion information (Knierim et al., 1995; Markus et al., 1995; Rubin et al., 2014), but no study has directly measured hippocampal head-directional modulation when vestibular-based signals are impaired.

Thus, the mechanisms governing hippocampal directional activity in rodents are unclear. We hypothesize that visual cues directly influence the activity of rodent hippocampal neurons to generate angular tuning, whereas vestibular cues are not required for directionality. This hypothesis is consistent with primate studies and thus bridges a long-standing gap between the

rodent (Andersen et al., 2006; Muller et al., 1994) and primate literature (Rolls and O'Mara, 1995; Rolls, 1999).

RESULTS

Head-Directional Modulation Is Present in Two-Dimensional RW

To test these hypotheses, we did a series of experiments and analyses. We first quantified (in 32 recording sessions) hippocampal spatial and head-directional modulation from 1,066 active (defined as cells with minimum mean firing rate of 0.2 Hz and with at least 100 spikes) dorsal CA1 pyramidal neurons (which were part of a previous study of hippocampal spatial selectivity [Aghajan et al., 2015]). Rats randomly foraged for reward on a two-dimensional platform in a RW environment that had rich distal visual cues and will henceforth be referred to as RW_{rich} (Figure 1A).

A common technique for quantifying head-directional modulation is to divide the number of spikes in each direction bin by the total time spent in that bin (Figure 1B; Taube, 2007). However, when neurons have spatially tuned responses, as is the case for hippocampal neurons in RW, this method provides incorrect estimates of angular tuning (Muller et al., 1994). For example, for a neuron with a place field at the edge of the maze, this method would yield an erroneous estimate of head-directional tuning due to non-uniform sampling of head angles within the place field (Figures 1B and S1; Muller et al., 1994). Various methods have been developed to overcome this confound (Burgess et al., 2005; Markus et al., 1995; Rubin et al., 2014). Here, we adopted the well-established generalized linear model (GLM) approach (see Experimental Procedures; Lepage et al., 2012; MacDonald et al., 2011; Nitz, 2012; Truccolo et al., 2005), which has several advantages. First, it provides an unbiased estimate of the simultaneous and independent contribution of spatial and head-directional modulation. Second, unlike other methods, head-directional modulation obtained with the GLM method is uninfluenced by behavioral biases within the place field, as verified using surrogate data with predetermined levels of spatial and angular modulation (see Experimental Procedures; Figure S1). Finally, this method provides an estimate of the fine structure of the respective tuning curves.

This method revealed a surprising finding: many neurons exhibited clear modulation by the rat's head direction (independent of the rat's body angle) in RW_{rich} (Figures 1C–1E and S2A; Experimental Procedures). Some neurons fired maximally for only one head direction and minimally elsewhere (Figures 1C and 1D), while others showed a multimodal response (Figure 1E). The degree of head-direction selectivity was assessed by computing the angular sparsity of head-directional firing rate maps (see Experimental Procedures). The statistical significance of head-directional modulation was assessed by bootstrapping methods. Cells with angular sparsity >95% of the control data (for the same cell) were considered significantly modulated (see Experimental Procedures). This method showed that 27% of neurons in RW_{rich} exhibited significant head-directional modulation, which is comparable to that in many parts of the head direction system, although the width of the angular tuning curves (full width at half maximum, $101.90^\circ \pm 3.35^\circ$) was wider (Boccara et al., 2010; Taube, 2007). Different place fields of the same neuron—with multiple fields—exhibited different levels of directional tunings (Figure S3), suggesting that directionality was a property of a place field, not of a neuron. This is also reminiscent of the results observed in double-rotation experiments, in which different fields of the same neuron responded differently to the rotation of certain cues (Knierim, 2002). These results show that rodent hippocampal neurons in RW indeed show significant head-directional modulation during two-dimensional random foraging, contrary to previous reports.

Robust Vestibular Cues Are Not Required for Hippocampal Directionality

The above results raise an important question: which sensory inputs could generate the head-directional modulation in our data? Two likely candidates are the visual and the vestibular modalities. To dissociate the two, we measured the activity of 719 (37 recording sessions) active dorsal hippocampal CA1 pyramidal neurons (Aghajan et al., 2015) during the same random foraging task in a two-dimensional VR environment (VR_{rich}). Here, the distal visual cues were identical to those in RW_{rich}, but the range of vestibular cues was minimized due to body fixation (Cushman et al., 2013). Despite impaired spatial selectivity (Aghajan et al., 2015), many neurons showed clear modulation by the direction of the rat's head with respect to the distal visual cues, which will be henceforth referred to as "head direction" (Figures 2 and S2B).

The observation that head-directional modulation was present in VR—where the range of vestibular cues is minimized (Figure 3)—suggests that vestibular cues are not required for hippocampal head-directional modulation. In fact, the angular speed—a good measure of the strength of vestibular inputs—at the time of occurrence of spikes had no effect on the fraction of significantly modulated neurons in not only VR, but also RW (Figure 3). Indeed, a similar fraction of neurons showed significant head-directional modulation in VR_{rich} (23%) and RW_{rich} (27%; Figure 4A).

These results are different from findings in the head-direction nuclei that require robust vestibular cues to generate directional selectivity (Taube, 2007). Additionally, neurons in VR_{rich} also had multimodal responses like in RW_{rich}, unlike neurons in the head-direction network, which have unimodal responses (Taube et al., 1990). The multimodality was greater in VR_{rich} than RW_{rich} (Figure 4B), which could account for the slightly lower proportion of cells with a significantly large mean vector length in the former (Figure S4). This observation motivates the use of sparsity as a measure for angular selectivity. Additionally, the width of the angular tuning curves in VR_{rich} ($85.41^\circ \pm 4.23^\circ$) was significantly (16%, $p = 5.13 \times 10^{-4}$) sharper than in RW_{rich}. Further, directionally tuned neurons had greater mean firing rates than the untuned neurons in VR_{rich} (Figure S5A), but not in RW_{rich}. Notably, angular sparsity strongly depends on the logarithm of number of spikes generated by a neuron (Figure S5B). When accounting for the differences in number of spikes across conditions, there was no significant difference in the angular sparsity of the ensemble of neurons between VR and RW ($p = 0.09$, two-way ANOVA; see Experimental Procedures).

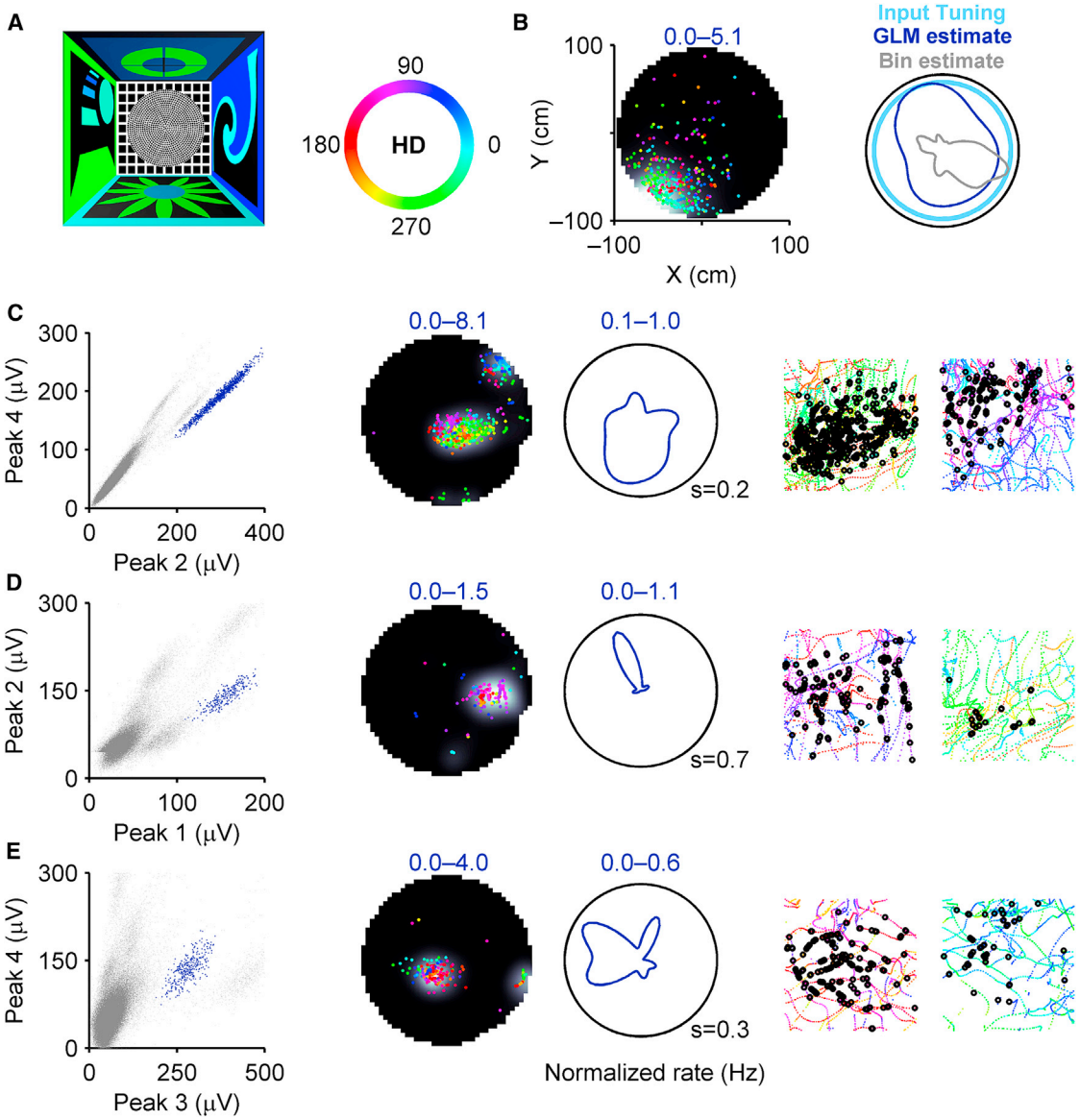

Figure 1. Presence of Head-Directional Modulation in Hippocampal Pyramidal Neurons in RW_{rich}

(A) (Left) A top-view schematic depicting a 300 × 300 cm room with four different visual cues on the walls and an elevated 100 cm radius platform at the center. (Right) A color wheel representing the mapping between head-directions and colors.

(B) (Left) Spatial firing rate of a surrogate (see Experimental Procedures) neuron (gray scale range indicated by numbers; lighter shades correspond to higher values here and throughout all figures) overlaid with the position of the rat when spikes occurred (colored dots). Each color represents a distinct head direction as shown in (A). The surrogate neuron's activity was constructed to have significant spatial selectivity, but no angular selectivity. (Right) Angular rate map of the same surrogate neuron estimated using the binning (gray) and GLM (blue) methods, along with the uniform input tuning (light blue). The GLM method provided an accurate estimate of the input, but the binning method overestimated the angular tuning due to behavioral bias. See also Figure S1.

(C) (Left) All unclustered (gray dots) and clustered spike amplitudes from an isolated neuron (blue dots) on two different projections of a tetrode in RW_{rich}. (Center) Spatial and angular rate maps of a cell (same convention as in B). Numbers in color indicate range here and throughout unless noted otherwise. The number at the lower-right corner of the polar plot is the sparsity of the angular rate map. (Right) Rat's color-coded trajectory and his position at the time of spikes (black circles) for movement in the direction of maximal (left) and minimal (right) firing, respectively.

(D and E) Same as (C) for two other cells in RW_{rich}. All rate maps were computed using the GLM method here and throughout unless otherwise noted. See also Figure S2A.

All cells in this figure showed significant angular modulation as verified through bootstrapping methods (see Experimental Procedures). See also Figure S3.

We then quantified the spatial modulation of neural responses in both RW_{rich} and VR_{rich} using the rate maps obtained from the GLM method. We found a large proportion of cells with significant spatial selectivity in RW_{rich}, but not in VR_{rich} (Figure 4C), consistent with previous results obtained using the binning method (Aghajan et al., 2015). Although comparable proportions

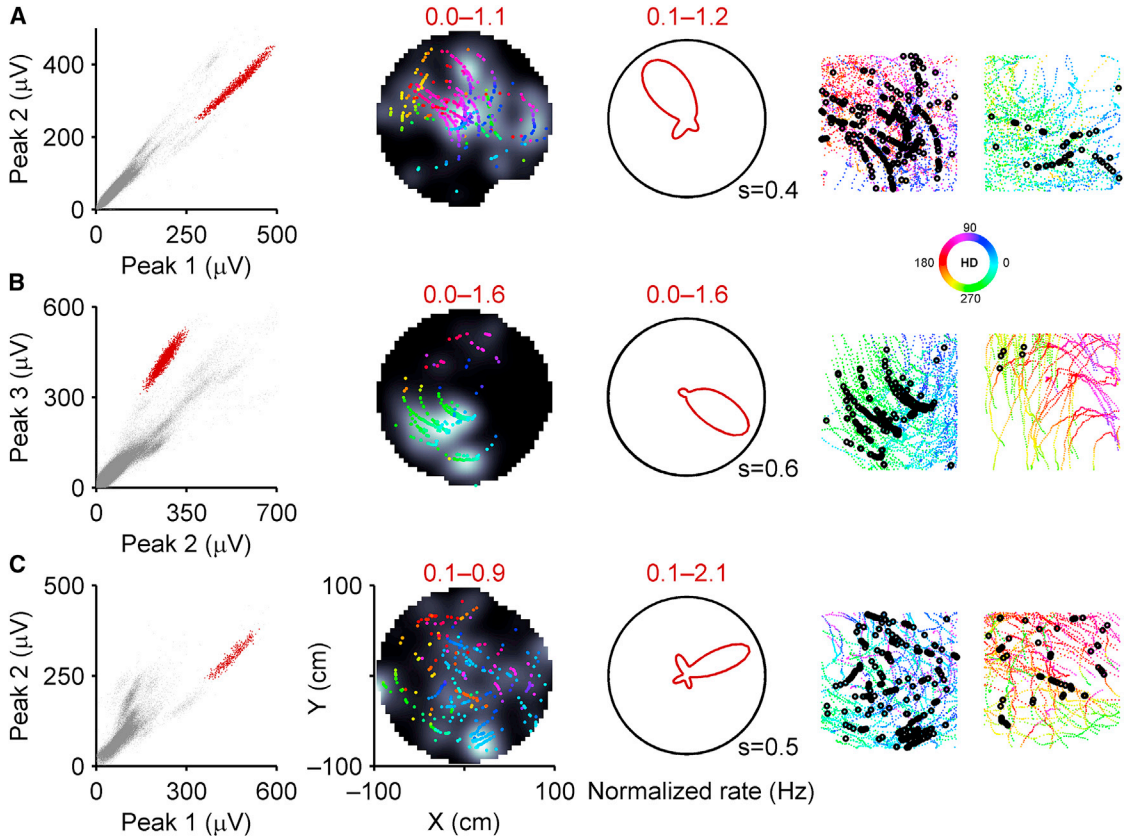

Figure 2. Presence of Head-Directional Modulation in Hippocampal Pyramidal Neurons in VR_{rich}

(A–C) Three well-isolated neurons showing significant head-directional modulation in VR_{rich} (same conventions as in Figure 1). All cells in these three panels showed significant angular modulation, as verified through bootstrapping methods (see Experimental Procedures). See also Figures S2B, S4, and S5.

of cells had significant head-directional modulation, this was not the case for spatial modulation, which suggests a decoupling of the mechanisms of spatial and directional tuning. Consistently, the presence or absence of head-directional modulation had no effect on the percentage of spatially modulated neurons in both RW_{rich} and VR_{rich} (Figure S5C). Further, spatial sparsity also depended strongly on the logarithm of number of spikes generated by a neuron (Figure S5D). When this was taken into account, there was a significant difference between the spatial sparsity of rate maps between VR and RW ($p = 1.7 \times 10^{-6}$, two-way ANOVA; see Experimental Procedures)

Visual Cues Exert a Causal and Predictable Influence on Hippocampal Directional Responses

What other mechanism could generate angular modulation? Either it is internally generated (MacDonald et al., 2011; Pastalkova et al., 2008; Peyrache et al., 2015) or driven by specific visual cues (Rolls and O'Mara, 1995; Rolls, 1999). To disambiguate these possibilities, we generated a virtual world where distal visual cues were entirely eliminated (VR_{blank}) (Figure 5A; Experimental Procedures). The circular platform in the virtual environment, which was the only visual cue present, provided optic flow information but had no spatial or angular information. The rats' behavior in VR_{blank} was comparable to that in VR_{rich} with visually distinct walls (comparable running speeds and distribution of occupancy across the platform). Very few hippocampal neurons (6%) showed significant head-directional modulation in this case (Figures 5B and 5I), close to the chance level of 5%.

The absence of head-directional modulation in VR_{blank} may result from a lack of anchoring visual cues (Blair and Sharp, 1996) or a lack of optic flow created by distal visual cues that could potentially be integrated to generate directional tuning. To address this, we performed another experiment in which all of the virtual walls had the same visual texture with high contrast and spatial frequency ($VR_{symmetric}$), thus providing strong optic flow information but no angular information (Figure 5C; Experimental Procedures). The virtual platform was placed in a larger room where each wall was 450 cm away from the platform center, which ensured that the distance from the walls provided minimal spatial and angular information. Here too, only a small percentage of neurons (7%) exhibited significant head-directional modulation, similar to VR_{blank} and close to chance level (Figures 5D and 5I).

While internal mechanisms and optic flow may still modulate the degree of angular tuning, these experiments show that directional modulation is not generated by these mechanisms alone. This leaves open the possibility that head-directional modulation

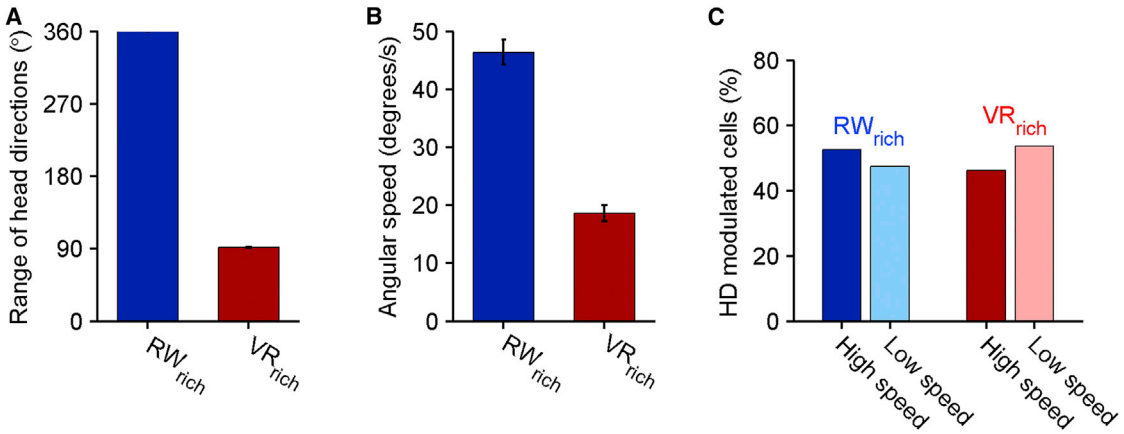

Figure 3. Directional Modulation Was Independent of Angular Speed and Range of Vestibular Inputs

(A) For 32 (37) sessions in RW (VR), the range of head-directions with respect to the experimental room in RW (359.99° ± 0.00°) was significantly higher than that in VR (91.67° ± 0.93°, $p = 2.2 \times 10^{-21}$).

(B) Angular speed in VR (18.63 ± 1.37 degrees/s, n = 37 sessions) was significantly reduced (60%, $p = 3.6 \times 10^{-11}$) compared to RW sessions (46.40 ± 2.12 deg/s, n = 32 sessions).

(C) For each neuron, the average angular speed at the time of occurrence of spikes was computed. This value was then used to classify a neuron into either high or low angular speed category, compared to the mean angular speed in RW (49.60 deg/s) and VR (19.91 deg/s). Nearly equal proportions of directionally modulated cells in RW 50.68% (49.32%) and in VR 47.12% (51.88%) belonged to the high (low) speed categories, respectively.Throughout the figure legends, values are reported as mean ± SEM, the statistical significance for comparisons was computed using Wilcoxon rank-sum test.

is generated by the angular information contained in the distal visual cues. To confirm this hypothesis, we performed another experiment in which the virtual world was strongly visually polarized. In this condition, there was just one high-contrast wall, 450 cm from the center of the platform, subtending a 90°angle ($VR^{wide}_{polarized}$; Figure 5E; Experimental Procedures). This polarizing cue had no other spatial information and was identical to the walls used in the symmetric world. Here, 31% of hippocampal neurons showed significant head-directional modulation (Figures 5F, 5I, and S6), which is a greater fraction than in all other conditions but comparable to that in RW_{rich} and VR_{rich}. Remarkably, the directional tuning curves of many neurons were much narrower (77.35° ± 3.62°) than the sole, 90° wide polarizing cue.

Is there a lower bound on the width of the angular tuning curves? To address this, we conducted another experiment in which the sole polarizing cue was very narrow (11°), thus providing high angular information in the direction of the cue while leaving the majority of the maze blank ($VR^{narrow}_{polarized}$; Figure 5G; Experimental Procedures). A large proportion (15%) of neurons had significant head-directional tuning in this condition as well (Figures 5H, 5I, and S7). For neurons with significant head-directional tuning, the width of the tuning curves (65.29° ± 4.97°) was significantly ($p = 6.5 \times 10^{-3}$,Wilcoxon rank-sum test) narrower than in $VR^{wide}_{polarized}$ (Figure 5J) but much wider than the 11° polarizing cue, indicating a lower bound on the width of hippocampal angular tuning curves. Further, the fraction of neurons showing significant head-directional modulation (15%) was considerably lower than in $VR^{wide}_{polarized}$ (Figure 5I), perhaps because the narrow visual cue is visible to the rat for a smaller fraction of time than the wider polarizing cue, hence modulating a smaller percentage of neurons. Notably, in all RW and VR experiments, several angular rate maps showed multimodal responses despite considerable differences in the nature of visual cues (Figure 5K), suggesting underlying internal mechanisms.

We then asked whether the head-directional modulation of hippocampal neurons is stable and whether the stability depends on the experimental condition (Figure 6). Tuning curves of neurons with significant head-directional modulation were significantly stable across the experimental session in all four conditions (RW_{rich} $p = 8.7 \times 10^{-46}$, VR_{rich} $p = 1.1 \times 10^{-23}$, $VR^{wide}_{polarized}$ $p = 1.1 \times 10^{-21}$, and $VR^{narrow}_{polarized}$ $p = 1.3 \times 10^{-11}$, Wilcoxon signed-rank test) (Figures 6A–6D). The tuning curves were more stable ($p = 9.2 \times 10^{-7}$) in RW_{rich} than in VR_{rich} (Figures 6E and 6F). This could be due to the presence of other directionally informative multisensory cues in RW, such as distal odors and sounds, and their consistent pairing with visual cues, resulting in higher stability. On the other hand, the tuning curves were more stable in the polarized VR experiments than in either of the rich conditions (Figures 6E and 6F), indicating that there may be competing influences of multiple cues within each modality in the rich conditions.

Visual Cues Bias Hippocampal Ensemble Response

These results demonstrate that specific aspects of visual cues modulate the angular tuning of individual neurons; could they also influence the ensemble response? To address this, we investigated the activity of the head-directionally modulated neurons on a population level under the four different conditions. For each neuron, the direction of maximum firing was computed from its angular rate map and was designated as its preferred direction (Figures 7A–7D; see Experimental Procedures). We then computed the distribution of these preferred directions and the degree of angular bias of the population for each condition. There was no significant angular bias, as indicated by the circular

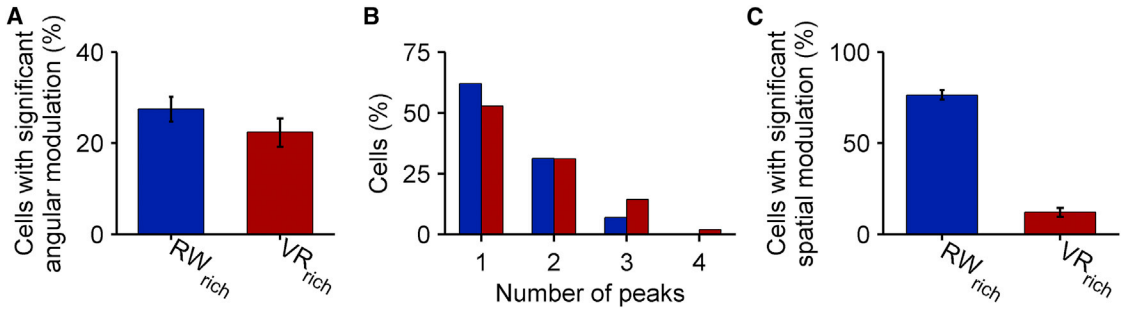

Figure 4. Similar Levels of Significant Head-Directional Modulation in RW_{rich} and VR_{rich}

(A) The population of neurons in VR_{rich} (red, n = 719; 37 sessions) and RW_{rich} (blue, n = 1066; 32 sessions) had comparable proportions of cells with statistically significant angular sparsity; 27, [25, 30]% (23, [19, 26]%) of cells in RW_{rich} (VR_{rich}) showed significant head-directional modulation (see Experimental Procedures). See also Figure S5.

(B) Head-directionally modulated neurons in VR_{rich} were significantly more multimodal (1.65 ± 0.06 peaks, $p = 1.4 \times 10^{-2}$) than RW_{rich} cells (1.45 ± 0.04 peaks). See also Figures S2, S4.

(C) In contrast to angular sparsity, far fewer neurons (12, [10, 15]%) in VR_{rich} had significant spatial sparsity compared to RW_{rich} (76, [74, 79]%).

Rayleigh test, in both RW_{rich} ($p = 0.1$) and VR_{rich} ($p = 0.4$), and the two distributions were not significantly different from each other ($p = 1$, circular Kuiper test; Figures 7E and 7F). The lack of population bias in the rich conditions is likely due to the presence of multiple visual cues on all walls, each contributing to tuning toward different directions.

Indeed, in $VR^{wide}_{polarized}$ with only one visual cue, the population was significantly biased ($p = 0.04$, circular V test) toward the prominent visual cue (Figure 7G). The directional bias of the population was strongest in $VR^{narrow}_{polarized}$ such that the distribution of preferred orientations was significantly different from a uniform distribution ($p = 3.6 \times 10^{-3}$ Rayleigh test) and, in addition, was oriented toward the narrow visual cue ($p = 4.3 \times 10^{-4}$, circular V test; Figure 7H). There was an apparent reduction in the number of cells with preferred direction directly toward the narrow polarizing cue, and for some cells, the preferred direction was opposite to the visual cue, which could arise due to release from potent, feed-forward, and lateral inhibition in CA1 (Hahn et al., 2006, 2007).

DISCUSSION

These results demonstrate that, during two-dimensional random foraging, rodent hippocampal CA1 neurons show significant modulation as a function of head direction with respect to the surrounding distal visual cues in both real and virtual worlds. This directional modulation does not require robust vestibular cues, whereas angularly informative visual cues are sufficient for its generation. Additionally, the proportion of neurons with significant directional modulation, the direction of their tuning, and the directional tuning curve width are all strongly influenced by the degree of angular information in the distal visual cues, both at the neuronal and ensemble level, thereby demonstrating the causal influence of visual cues on rodent hippocampal directional responses.

Our demonstration of significant head-directional modulation of hippocampal neurons' activity during random foraging in two dimensions in RW is contrary to the commonly held belief that head-directional modulation is absent in this condition in rodents (Andersen et al., 2006; Muller et al., 1994). There have been a few conflicting reports about hippocampal head-directional selectivity in rats (Markus et al., 1995; Wiener et al., 1989) and bats (Rubin et al., 2014; Ulanovsky and Moss, 2011) in open fields. Directional selectivity in bats was initially thought to be generated by visual cues (Ulanovsky and Moss, 2011) but was later ascribed to vestibular cues and spatial selectivity (Rubin et al., 2014). Additionally, a few studies have reported directionally selective responses in the primate hippocampus (Rolls and O'Mara, 1995; Rolls, 1999). Our results about directionally selective responses in RW are consistent with these primate studies. There could be several reasons why we found strong directional selectivity in this condition when previous studies failed to find such responses. First, unlike most studies, we used prominent, rich visual cues that could elicit visually evoked responses. Second, we used a large (200 cm diameter) open platform placed in a large room (300 × 300 cm), where we attempted to eliminate nonspecific cues, in contrast to most studies that use a small enclosure with nearby walls, which could provide nonspecific cues that could interfere with the visual cues. Further, we employed analysis techniques that eliminated the possibility that the directionality we observed was influenced by spatially selective responses or behavioral artifacts. Finally, we estimated angular tuning by computing angular sparsity, which is more robust to estimating the selectivity of multimodal responses than the commonly used mean vector length.

Notably, we found comparable levels of directional responses in both visually rich RW and in VR, where the vestibular cues were minimized. This is in contrast to the commonly held belief that directional responses in rodent hippocampus and related systems require robust vestibular cues (Andersen et al., 2006; Knierim et al., 1995; Markus et al., 1995; Stackman et al., 2002) but is consistent with visually evoked direction-selective responses in primates without vestibular cues (Rolls and O'Mara, 1995; Rolls, 1999).

These results demonstrate that visual cues alone are sufficient to generate rodent hippocampal direction selectivity. To determine the causal influence of the nature of visual cues on this selectivity, we did a series of experiments in VR. This isolation

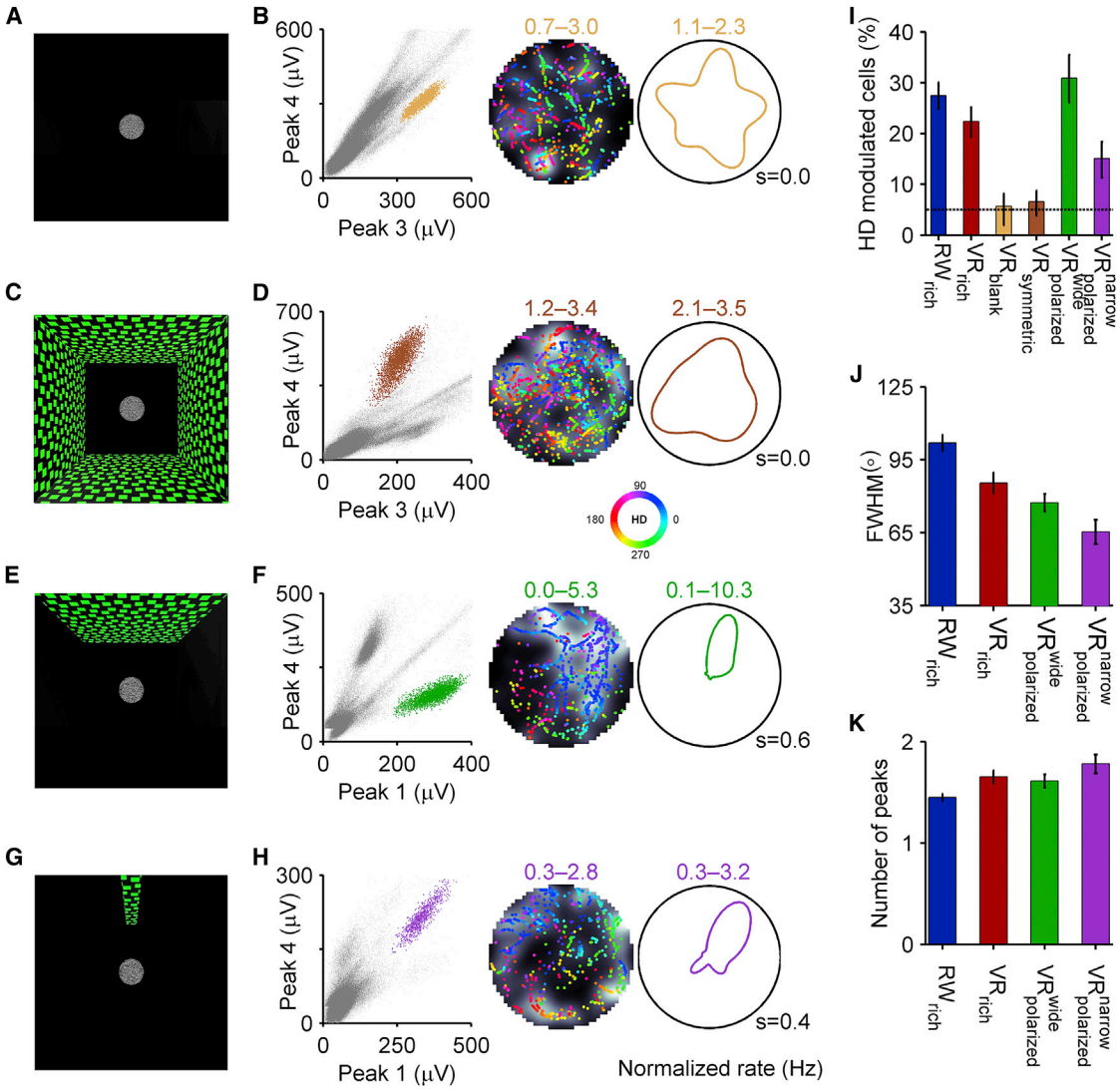

Figure 5. Causal and Predictable Influence of Visual Cues on Directional Modulation of Neurons

(A) Top-down schematic of VR task with a 100 cm radius circular platform with no distal visual cues (VR_{blank}).

(B) (Left) Spikes from an isolated neuron (mustard dots) in VR_{blank} (same convention as in Figure 1). (Center and right) Spatial and angular firing rate of this neuron (same conventions as in Figure 1).

(C) Top-down schematic of VR task with symmetric cues located 450 cm away from the center of the circular platform ($VR_{symmetric}$).

(D) Same as in (B) but in $VR_{symmetric}$. Neurons in both (B) and (D) do not show significant angular sparsity.

(E) Top-down schematic of VR task with a single wide polarizing visual cue 450 cm away from the center (90° visual angle) of the platform ($VR^{wide}_{polarized}$).

(F) Same as (B) and (D) but in $VR^{wide}_{polarized}$. See also Figure S6.

(G) Top-down schematic of VR task with a narrow polarizing cue 450 cm away from the center (11° visual angle) of the circular table ($VR^{narrow}_{polarized}$).

(H) Same as (B), (D), and (F) but in $VR^{narrow}_{polarized}$. See also Figure S7. Note that the neurons shown in both (F) and (H) exhibit strong head-directional modulation.

(I) The percentages of cells with significant head-directional modulation was 27, [25, 30]% in RW_{rich} (293 out of 1066 cells; 32 sessions); 23, [19, 26]% in VR_{rich} (162 of 719 cells; 37 sessions); 6, [3, 9]% in VR_{blank} (13 of 230 cells; 8 sessions); 7, [4, 9]% in $VR_{symmetric}$ (28 of 426 cells; 10 sessions); 31, [26, 38]% in $VR^{wide}_{polarized}$ (121 of 391 cells; 14 sessions) and 15, [12, 19]% in $VR^{narrow}_{polarized}$ (64 of 424 cells; 20 sessions). The black horizontal line indicates the chance level of 5%.

(J) Full width at half max (FWHM) of the angular rate maps for head-directionally modulated neurons in different conditions was as follows: RW_{rich} (101.90° ± 3.35°), VR_{rich} (85.41° ± 4.23°), $VR^{wide}_{polarized}$ (77.35° ± 3.62°), and $VR^{narrow}_{polarized}$ (65.29° ± 4.97°). The tuning curves in RW_{rich} were significantly wider than all other VR conditions ($p = 5.1 \times 10^{-4}$ versus VR_{rich}, $p = 3.3 \times 10^{-5}$ versus $VR^{wide}_{polarized}$, and $p = 5.3 \times 10^{-8}$ versus $VR^{narrow}_{polarized}$). Within VR conditions, $VR^{narrow}_{polarized}$ had significantly narrower tuning curves with respect to VR_{rich} ($p = 3.7 \times 10^{-3}$) and $VR^{wide}_{polarized}$ ($p = 6.5 \times 10^{-3}$).

(K) Angular rate maps in all VR conditions were significantly more multimodal (1.65 ± 0.07 peaks, $p = 1.4 \times 10^{-2}$ in VR_{rich}; 1.61 ± 0.07, $p = 3.3 \times 10^{-2}$ in $VR^{wide}_{polarized}$; 1.78 ± 0.09, $p = 4.8 \times 10^{-4}$ in $VR^{narrow}_{polarized}$) than RW_{rich} (1.45 ± 0.04 peaks). Values are reported as mean ± SEM, the p values are obtained by Wilcoxon rank-sum test, and percentages and numbers in brackets correspond to maximum likelihood estimates and 95% confidence intervals, unless noted otherwise.

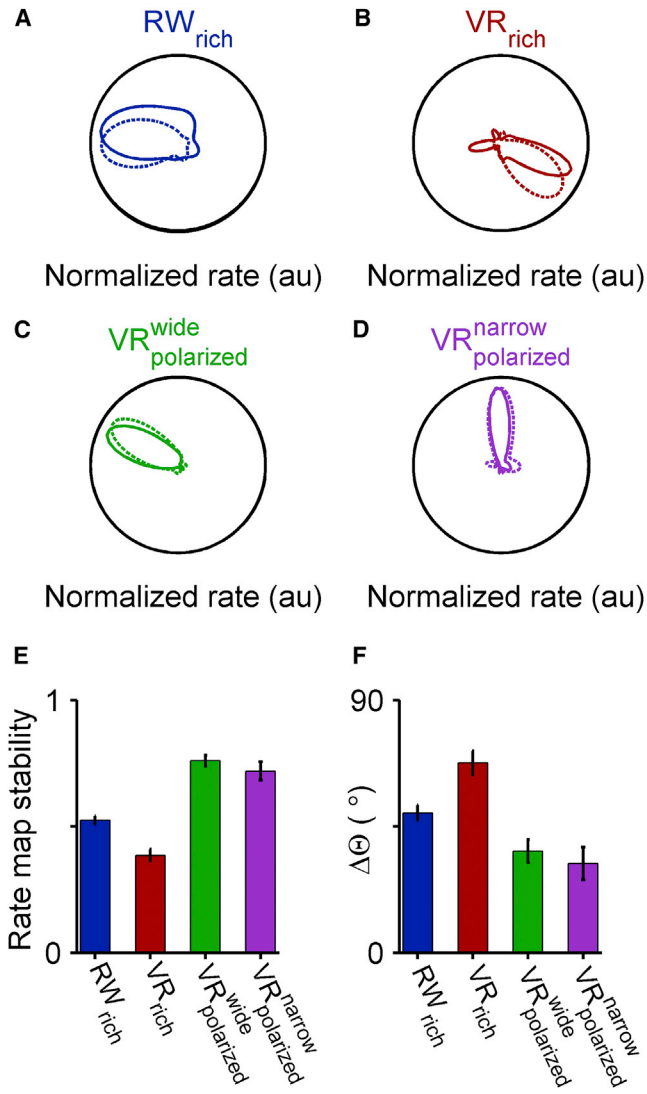

Figure 6. Stability of Angular Rate Maps for Head-Directionally Modulated Neurons

(A–D) Four directionally tuned cells with stable angular firing in the first half (solid colored lines) and second half (dashed colored lines) of the recording session. The peak rates are normalized for ease of comparison.

(E) Stability of the head-directional modulation (computed as the pairwise correlation between the angular rate maps in the first and second halves) in RW_{rich} (0.52 ± 0.02, n = 293) was significantly greater than VR_{rich} (0.39 ± 0.02, n = 162, p = 9.2 × 10^{-7}, Wilcoxon rank-sum test here and throughout figure legend) but significantly smaller than $VR^{wide}_{polarized}$ (0.76 ± 0.02, n = 121, p = 8.5 × 10^{-19}) and $VR^{narrow}_{polarized}$ (0.72 ± 0.04, n = 64, p = 2.3 × 10^{-9}). Angular rate map stability was not significantly different between $VR^{wide}_{polarized}$ and $VR^{narrow}_{polarized}$ (p = 0.35).

(F) As an alternate measure of stability, we computed the absolute value of the circular distance between the preferred directions (defined as the direction of peak firing) in the two session halves. This method also resulted in a similar trend with $VR^{wide}_{polarized}$ (36.23° ± 4.06°) and $VR^{narrow}_{polarized}$ (31.83° ± 5.82°) showing identical levels of drift of the preferred directions (p = 0.15), both smaller than the amount of angular drift in RW_{rich} (49.85 ± 2.83°, p = 7.2 × 10^{-5} and p = 7.4 × 10^{-6} respectively) and VR_{rich} (67.65 ± 4.34°, p = 6.3 × 10^{-8} and p = 9.9 × 10^{-8} respectively).

of visual cues is not possible in RW since nonspecific cues (Battaglia et al., 2004), including vestibular cues, are invariably present in RW and could confound interpretation. We found that the amount of angular information in the visual cues directly determined the proportion of hippocampal neurons that had significant directional selectivity. Removing angular information in the visual cues eliminated directional selectivity of hippocampal responses. Compared to the visually rich VR, making the visual cues angularly concentrated resulted in sharpening of the head-directional tuning curves. In addition, narrowing of the same polarizing visual cue had a predictable effect: fewer neurons were angularly tuned, but their directional tuning curves were even sharper. These results show that visual cues play a causal and predictable role in determining rodent hippocampal directional responses. While these results are novel for rodents, they are consistent with extensive primate literature showing visually evoked selective responses in the primate hippocampal formation (Ekstrom et al., 2003; Killian et al., 2012; Rolls, 1999; Suzuki et al., 1997). However, we found that the angular tuning curves were wider than the visual stimulus. This increased width could arise due to mechanisms of persistent activity (Aghajan et al., 2015; Hahn et al., 2012; Yoshida and Hasselmo, 2009) and could improve the angular accuracy of the ensemble of neurons by improving signal-to-noise ratio of the ensemble (Zhang and Sejnowski, 1999).

In addition, we found that visual cues influence not only the angular responses of individual neurons, but also the hippocampal ensemble response. Concentration of visual cues in one part of the wall caused the ensemble to become preferentially biased in that direction, demonstrating that hippocampal responses were visually evoked. This could explain why there was no ensemble bias in the rich conditions in which different neurons fire preferentially to different visual features on the walls.

Hence, we hypothesize that, while the hippocampal formation receives directional signals from the vestibular cue-dependent head-direction system, it must also be receiving directional information from a pathway that does not require the vestibular signal but could instead be driven by visual cues, such as the entorhinal cortex (Alexander and Nitz, 2015; Deshmukh and Knierim, 2011; Winter et al., 2015). For example, layer 3 of medial entorhinal cortex, which is a primary source of input to the dorsal CA1 and which drives CA1 neurons (Hahn et al., 2012), could contain a subset of the head-directionally tuned neurons that are visually driven and that maintain significant angular selectivity even in our VR setup, thus contributing to the directional tuning of CA1 neurons. By showing the presence of significant directional tuning in this condition, our findings narrow the gap between the presence of directionality on linear tracks in real (McNaughton et al., 1983) and virtual worlds (Ravassard et al., 2013) but its apparent absence during random foraging in two dimensions (Andersen et al., 2006; Muller et al., 1994). Further studies are needed to determine whether rodent hippocampal responses are distributed in the allocentric (O'Keefe and Dostrovsky, 1971), egocentric (Alexander and Nitz, 2015; Nitz, 2006; Whitlock et al., 2012), or retinotopic (Rolls, 1999) frames of reference. Further, our experiments do not rule out the possibility that other sensory, behavioral, and internal cues could also influence hippocampal directionality.

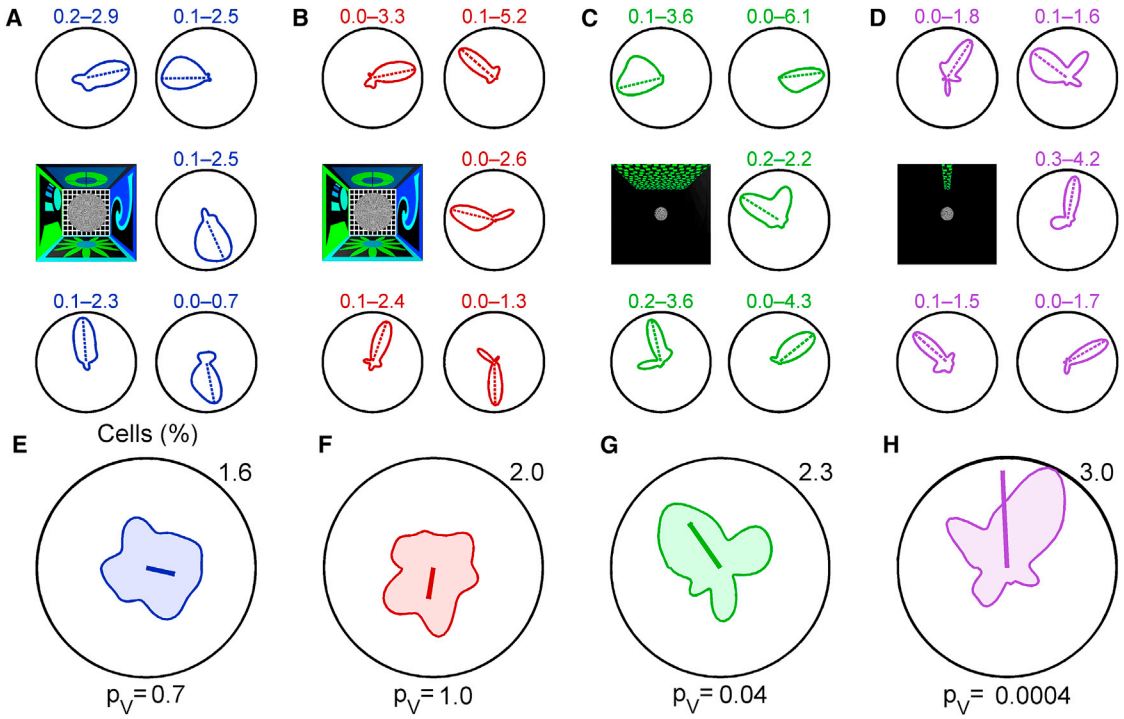

Figure 7. Visual Cues Bias the Neural Ensemble

(A) Five example cells in RW_{rich} with significant directional tuning. The numbers indicate firing rate range. The dashed line corresponds to the preferred direction, i.e., the direction of maximum firing. The schematic in the middle-left indicates the experimental condition.

(B–D) Same as in (A) but in VR_{rich}, $VR^{wide}_{polarized}$, and $VR^{narrow}_{polarized}$ conditions, respectively. All cells in these panels showed significant angular modulation, as shown by the bootstrapping method (see Experimental Procedures).

(E) Distribution of preferred direction of neurons in RW_{rich} is not significantly different from a uniform distribution ($p = 0.1$, circular Rayleigh test) and is not significantly biased ($p_V = 0.7$, circular V test), and the mean vector length of the ensemble (0.09) was smaller than 95% of the shuffles (see Experimental Procedures; circular mean ± circular SEM of the distribution = 347.80° ± 4.52°, n = 293). The number on the upper-right indicates the maximum value of the distribution. The thick blue line originating at the center of the polar plot represents both the direction (347.80°) and the magnitude (0.09) of the mean vector length of the preferred directions of the population (scaled by a factor of 5 for clarity).

(F) Same as in (E) but for VR_{rich}. The distribution of preferred directions of neurons in VR_{rich} did not show any significant bias ($p = 0.4$, Rayleigh test of uniformity; $p_V = 1$, circular V test for angular bias), and the mean vector length of the ensemble (0.1) was not significantly different from chance (circular mean ± circular SEM of the distribution = 260.91° ± 6.07°, n = 162). Additionally, this distribution was not significantly different from that in RW_{rich} ($p = 1$, circular Kuiper test).

(G) The ensemble of head-directionally modulated neurons in $VR^{wide}_{polarized}$ preferentially fired toward the visual cue ($p_V = 0.04$, circular V test), and the mean vector length of the population (0.17) was greater than chance (circular mean ± circular SEM of the distribution = 124.99° ± 8.18°, n = 121). Note the direction (124.99°) and the longer magnitude (0.17) of the thick green line compared to (E) and (F).

(H) On the population level, neurons in $VR^{narrow}_{polarized}$ (92.68° ± 8.51°, n = 64, circular mean ± circular SEM) were biased toward the narrow cue ($p_V = 0.04$, circular V test) and further indicated by the magnitude (0.29, significantly greater than chance) of the mean vector length of the ensemble (thick purple line) compared to all other conditions, and this distribution is significantly different from a uniform distribution ($p = 3.6 \times 10^{-3}$ Rayleigh test).

The intact head-directional modulation observed here is in contrast to the large reduction in spatial selectivity in VR (Aghajan et al., 2015). Thus, the mechanisms of spatial and directional selectivity can be dissociated, in that visual cues are sufficient to generate the latter, but not the former. Further, these results are also consistent with human and nonhuman primate studies showing the presence of angular selectivity independent of spatial selectivity (Ekstrom et al., 2003; Jacobs et al., 2010; Ono et al., 1993; Rolls, 1999).

Thus, our results bridge the long-standing gap between the primate and rodent studies by showing visually evoked, directional responses in the rodents regardless of vestibular cues. These results could potentially resolve the apparent paradox: if the hippocampus is required for navigation (Morris, 1984), how can rats (Cushman et al., 2013), humans, or nonhuman primates navigate with only visual cues and without robust hippocampal spatial selectivity (Aghajan et al., 2015; Jacobs et al., 2010; Rolls, 1999)? We hypothesize that the angular selectivity of hippocampal neurons reported here combined with their selectivity to distance traveled (Aghajan et al., 2015; Ravassard et al., 2013), and the experiential plasticity of hippocampal receptive fields (Mehta, 2015; Mehta et al., 2000, 1997) could mediate spatial navigation.

EXPERIMENTAL PROCEDURES

Five adult male Long-Evans rats foraged for randomly scattered rewards in RW and various VR tasks. Four rats ran in visually similar RW and VR tasks

with environments identical in size (300 × 300 cm room with a 200 cm diameter, elevated circular platform at the center). In addition, three rats ran in four other VR tasks with different distal visual features on a 200 cm diameter platform to determine their influence of hippocampal firing as follows: (1) a room with no distal visual cues; (2) a room with angularly symmetric cues with high spatial contrast positioned 450 cm away from the center; (3) a similar environment as in (2) but with only one high-contrast cue subtending a visual angle of 90° at the center; and (4) a similar environment as in (3) but with the visual cue subtending an angle of only 11° at the center.

At all locations on the platform, the individual visual features (green squares) in the visual cues in 2–4 above subtended an angle slightly >4° separated by ~4° of blank space. Since rats' Vernier acuity is about 1°, this ensured that the rats would be able to see this high-contrast texture from all locations on the maze and in mazes 2–4.

Electrophysiological data were collected using bilateral hyperdrives with 22 tetrodes from dorsal CA1 (Aghajan et al., 2015; Ravassard et al., 2013). All procedures were in accordance with NIH-approved protocols. Spatial and head-directional modulations were computed using a GLM framework (Kraus et al., 2013; Lepage et al., 2012; MacDonald et al., 2011; Nitz, 2012; Truccolo et al., 2005). Throughout the figure legends, the statistical significance for comparisons was computed using Wilcoxon rank-sum test, and numbers in brackets correspond to 95% confidence intervals unless otherwise stated. All pooled values are presented as mean ± SEM unless stated otherwise. The statistical significance of angular modulation was assessed using a bootstrapping procedure for each cell. See Supplemental Experimental Procedures for details.

SUPPLEMENTAL INFORMATION

Supplemental Information includes Supplemental Experimental Procedures and seven figures and can be found with this article online at http://dx.doi.org/10.1016/j.cell.2015.12.015.

AUTHOR CONTRIBUTIONS

Conceptualization, L.A., Z.M.A., and M.R.M.; Methodology, L.A., C.V., and M.R.M.; Software, Z.M.A. and J.J.M.; Formal Analysis, Z.M.A.; Investigation, L.A. and C.V.; Writing – Original Draft, L.A., Z.M.A., J.J.M., and M.R.M.; Writing – Review & Editing, L.A., Z.M.A., J.J.M., and M.R.M.; Visualization, Z.M.A.; Supervision, M.R.M.; Project Administration: M.R. M.; Funding Acquisition, M.R.M.

ACKNOWLEDGMENTS

We thank B. Popeney for help with behavioral training, J. Cushman and N. Agarwal for help with electrophysiology, P. Ravassard and A. Kees for technical support and help with surgeries, and B. Willers and V. Sagar for discussions on analysis methods. This work was supported by grants to M.R.M. from NIH 5R01MH092925-02 and from the W.M. Keck Foundation. Results presented in this manuscript were uploaded to the preprint server BioRxiv (http://biorxiv.org/lookup/doi/10.1101/017210).

Received: August 7, 2015
Revised: October 29, 2015
Accepted: December 1, 2015
Published: December 17, 2015

REFERENCES

Aghajan, Z.M., Acharya, L., Moore, J.J., Cushman, J.D., Vuong, C., and Mehta, M.R. (2015). Impaired spatial selectivity and intact phase precession in two-dimensional virtual reality. Nat. Neurosci. *18*, 121–128.

Alexander, A.S., and Nitz, D.A. (2015). Retrosplenial cortex maps the conjunction of internal and external spaces. Nat. Neurosci. *18*, 1143–1151.

Andersen, P., Morris, R., Amaral, D., Bliss, T., and O'Keefe, J. (2006). The hippocampus book (Oxford University Press).

Battaglia, F.P., Sutherland, G.R., and McNaughton, B.L. (2004). Local sensory cues and place cell directionality: additional evidence of prospective coding in the hippocampus. J. Neurosci. *24*, 4541–4550.

Blair, H.T., and Sharp, P.E. (1996). Visual and vestibular influences on head-direction cells in the anterior thalamus of the rat. Behav. Neurosci. *110*, 643–660.

Boccara, C.N., Sargolini, F., Thoresen, V.H., Solstad, T., Witter, M.P., Moser, E.I., and Moser, M.B. (2010). Grid cells in pre- and parasubiculum. Nat. Neurosci. *13*, 987–994.

Burgess, N., Cacucci, F., Lever, C., and O'keefe, J. (2005). Characterizing multiple independent behavioral correlates of cell firing in freely moving animals. Hippocampus *15*, 149–153.

Calton, J.L., Stackman, R.W., Goodridge, J.P., Archey, W.B., Dudchenko, P.A., and Taube, J.S. (2003). Hippocampal place cell instability after lesions of the head direction cell network. J. Neurosci. *23*, 9719–9731.

Cushman, J.D., Aharoni, D.B., Willers, B., Ravassard, P., Kees, A., Vuong, C., Popeney, B., Arisaka, K., and Mehta, M.R. (2013). Multisensory control of multimodal behavior: do the legs know what the tongue is doing? PLoS ONE *8*, e80465.

Deshmukh, S.S., and Knierim, J.J. (2011). Representation of non-spatial and spatial information in the lateral entorhinal cortex. Front. Behav. Neurosci. *5*, 69.

Ekstrom, A.D., Kahana, M.J., Caplan, J.B., Fields, T.A., Isham, E.A., Newman, E.L., and Fried, I. (2003). Cellular networks underlying human spatial navigation. Nature *425*, 184–188.

Hahn, T.T.G., Sakmann, B., and Mehta, M.R. (2006). Phase-locking of hippocampal interneurons' membrane potential to neocortical up-down states. Nat. Neurosci. *9*, 1359–1361.

Hahn, T.T.G., Sakmann, B., and Mehta, M.R. (2007). Differential responses of hippocampal subfields to cortical up-down states. Proc. Natl. Acad. Sci. USA *104*, 5169–5174.

Hahn, T.T.G., McFarland, J.M., Berberich, S., Sakmann, B., and Mehta, M.R. (2012). Spontaneous persistent activity in entorhinal cortex modulates cortico-hippocampal interaction in vivo. Nat. Neurosci. *15*, 1531–1538.

Jacobs, J., Kahana, M.J., Ekstrom, A.D., Mollison, M.V., and Fried, I. (2010). A sense of direction in human entorhinal cortex. Proc. Natl. Acad. Sci. USA *107*, 6487–6492.

Killian, N.J., Jutras, M.J., and Buffalo, E.A. (2012). A map of visual space in the primate entorhinal cortex. Nature *491*, 761–764.

Knierim, J.J. (2002). Dynamic interactions between local surface cues, distal landmarks, and intrinsic circuitry in hippocampal place cells. J. Neurosci. *22*, 6254–6264.

Knierim, J.J., Kudrimoti, H.S., and McNaughton, B.L. (1995). Place cells, head direction cells, and the learning of landmark stability. J. Neurosci. *15*, 1648–1659.

Kraus, B.J., Robinson, R.J., 2nd, White, J.A., Eichenbaum, H., and Hasselmo, M.E. (2013). Hippocampal "time cells": time versus path integration. Neuron *78*, 1090–1101.

Lepage, K.Q., Macdonald, C.J., Eichenbaum, H., and Eden, U.T. (2012). The statistical analysis of partially confounded covariates important to neural spiking. J. Neurosci. Methods *205*, 295–304.

MacDonald, C.J., Lepage, K.Q., Eden, U.T., and Eichenbaum, H. (2011). Hippocampal "time cells" bridge the gap in memory for discontiguous events. Neuron *71*, 737–749.

Markus, E.J., Qin, Y.L., Leonard, B., Skaggs, W.E., McNaughton, B.L., and Barnes, C.A. (1995). Interactions between location and task affect the spatial and directional firing of hippocampal neurons. J. Neurosci. *15*, 7079–7094.

McNaughton, B.L., Barnes, C.A., and O'Keefe, J. (1983). The contributions of position, direction, and velocity to single unit activity in the hippocampus of freely-moving rats. Exp. Brain Res. *52*, 41–49.

Mehta, M.R. (2015). From synaptic plasticity to spatial maps and sequence learning. Hippocampus *25*, 756–762.

Mehta, M.R., Barnes, C.A., and McNaughton, B.L. (1997). Experience-dependent, asymmetric expansion of hippocampal place fields. Proc. Natl. Acad. Sci. USA *94*, 8918–8921.

Mehta, M.R., Quirk, M.C., and Wilson, M.A. (2000). Experience-dependent asymmetric shape of hippocampal receptive fields. Neuron *25*, 707–715.

Morris, R. (1984). Developments of a water-maze procedure for studying spatial learning in the rat. J. Neurosci. Methods *11*, 47–60.

Muller, R.U., and Kubie, J.L. (1987). The effects of changes in the environment on the spatial firing of hippocampal complex-spike cells. J. Neurosci. *7*, 1951–1968.

Muller, R.U., Bostock, E., Taube, J.S., and Kubie, J.L. (1994). On the directional firing properties of hippocampal place cells. J. Neurosci. *14*, 7235–7251.

Nitz, D.A. (2006). Tracking route progression in the posterior parietal cortex. Neuron *49*, 747–756.

Nitz, D.A. (2012). Spaces within spaces: rat parietal cortex neurons register position across three reference frames. Nat. Neurosci. *15*, 1365–1367.

O'Keefe, J., and Dostrovsky, J. (1971). The hippocampus as a spatial map. Preliminary evidence from unit activity in the freely-moving rat. Brain Res. *34*, 171–175.

O'Keefe, J., and Nadel, L. (1978). The hippocampus as a cognitive map (Oxford: Clarendon Press).

Ono, T., Nakamura, K., Nishijo, H., and Eifuku, S. (1993). Monkey hippocampal neurons related to spatial and nonspatial functions. J. Neurophysiol. *70*, 1516–1529.

Pastalkova, E., Itskov, V., Amarasingham, A., and Buzsáki, G. (2008). Internally generated cell assembly sequences in the rat hippocampus. Science *321*, 1322–1327.

Peyrache, A., Lacroix, M.M., Petersen, P.C., and Buzsáki, G. (2015). Internally organized mechanisms of the head direction sense. Nat. Neurosci. *18*, 569–575.

Ravassard, P., Kees, A., Willers, B., Ho, D., Aharoni, D., Cushman, J., Aghajan, Z.M., and Mehta, M.R. (2013). Multisensory control of hippocampal spatiotemporal selectivity. Science *340*, 1342–1346.

Rolls, E.T. (1999). Spatial view cells and the representation of place in the primate hippocampus. Hippocampus *9*, 467–480.

Rolls, E.T., and O'Mara, S.M. (1995). View-responsive neurons in the primate hippocampal complex. Hippocampus *5*, 409–424.

Rubin, A., Yartsev, M.M., and Ulanovsky, N. (2014). Encoding of head direction by hippocampal place cells in bats. J. Neurosci. *34*, 1067–1080.

Shapiro, M.L., Tanila, H., and Eichenbaum, H. (1997). Cues that hippocampal place cells encode: dynamic and hierarchical representation of local and distal stimuli. Hippocampus *7*, 624–642.

Stackman, R.W., Clark, A.S., and Taube, J.S. (2002). Hippocampal spatial representations require vestibular input. Hippocampus *12*, 291–303.

Suzuki, W.A., Miller, E.K., and Desimone, R. (1997). Object and place memory in the macaque entorhinal cortex. J. Neurophysiol. *78*, 1062–1081.

Taube, J.S. (2007). The head direction signal: origins and sensory-motor integration. Annu. Rev. Neurosci. *30*, 181–207.

Taube, J.S., Muller, R.U., and Ranck, J.B., Jr. (1990). Head-direction cells recorded from the postsubiculum in freely moving rats. I. Description and quantitative analysis. J. Neurosci. *10*, 420–435.

Truccolo, W., Eden, U.T., Fellows, M.R., Donoghue, J.P., and Brown, E.N. (2005). A point process framework for relating neural spiking activity to spiking history, neural ensemble, and extrinsic covariate effects. J. Neurophysiol. *93*, 1074–1089.

Ulanovsky, N., and Moss, C.F. (2011). Dynamics of hippocampal spatial representation in echolocating bats. Hippocampus *21*, 150–161.

Whitlock, J.R., Pfuhl, G., Dagslott, N., Moser, M.B., and Moser, E.I. (2012). Functional split between parietal and entorhinal cortices in the rat. Neuron *73*, 789–802.

Wiener, S.I., Paul, C.A., and Eichenbaum, H. (1989). Spatial and behavioral correlates of hippocampal neuronal activity. J. Neurosci. *9*, 2737–2763.

Winter, S.S., Clark, B.J., and Taube, J.S. (2015). Spatial navigation. Disruption of the head direction cell network impairs the parahippocampal grid cell signal. Science *347*, 870–874.

Yoshida, M., and Hasselmo, M.E. (2009). Persistent firing supported by an intrinsic cellular mechanism in a component of the head direction system. J. Neurosci. *29*, 4945–4952.

Zhang, K., and Sejnowski, T.J. (1999). Neuronal tuning: To sharpen or broaden? Neural Comput. *11*, 75–84.